



# Evaluation of the Antimicrobial Efficacy of a Large-Area Surface Dielectric Barrier Discharge on Food Contact Surfaces

Caterina Maccaferri<sup>1</sup> · Ana Sainz-García<sup>2</sup> · Filippo Capelli<sup>1</sup> · Matteo Gherardi<sup>1,3</sup> · Fernando Alba-Elías<sup>2</sup> · Romolo Laurita<sup>1,4</sup>

Received: 28 June 2023 / Accepted: 4 October 2023 / Published online: 20 October 2023  
© The Author(s) 2023

## Abstract

The food industry, as a consequence of globalization and in particular with the outbreak of the COVID-19 pandemic, is calling for additional measures to reduce the risks of contamination throughout the steps of the food chain. Several methods are used to avoid this problem, such as hot water or chemical procedures. However, they have some disadvantages like high economic costs or the fact that they are not eco-friendly technologies. For those reasons, novel strategies are being sought in order to substitute or work in synergy with conventional decontamination systems. Cold atmospheric pressure plasma (CAP) can be produced by many various sources for a wide range of different applications, including decontamination. In this study, a Large-Area Surface Dielectric Barrier Discharge plasma source has been used with the aim of inactivating *Staphylococcus epidermidis* inoculated on polypropylene food packaging samples inside a treatment chamber. Moreover, electrical and chemical analysis of the plasma source has been carried out, as well as temperature measurements. A homogenous distribution of the reactive species inside the treatment chamber was suggested, achieving almost 2 log of bacteria reduction for every plasma treatment. Finally, it was suggested that the inactivation rates reached were not caused by the thermal effect. Thus, it is strongly believed that CAP could be an eco-friendly, cheap, and sustainable technology for food packaging and food tools decontamination.

**Keywords** Surface dielectric barrier discharge · Food industry · Nuclear technology · Plasma technology · Atmospheric pressure cold plasma · Decontamination

## Introduction

Food safety is which has begun to call for additional actions aimed at circumscribing as far as possible the risk introduced by the presence of potentially contaminated individuals in food production and marketing environments [1]. In that way, food packaging

---

Caterina Maccaferri and Ana Sainz-García are contributed equally to this work.

---

Extended author information available on the last page of the article

plays a crucial role during the final steps of the food chain preserving food from undesirable microorganisms and maintaining the original taste and odor.

Moreover, there is a globalization trend in the food market, which is beneficial for the supply and availability of food [2]. However, this fact has some disadvantages, such as economic or biological issues. Regarding the latter situation, contamination of food packaging and processing materials by microorganisms is an upsurging problem that could cause foodborne diseases. Taking into account the global market, contaminated packaging is known to be a means of transport for spreading diseases. According to the World Health Organization, 23 million people become ill each year in Europe due to foodborne diseases, and 5000 die [3]. Regarding the most frequent microorganisms seen in the food industry, *Staphylococcus* spp., *Listeria* spp., *E. coli*, *S. cerevisiae*, norovirus or anisakis are some of them [4, 5].

Traditional methods for the removal and inactivation of surface-attached pathogens from food contact surfaces are based on thermal, chemical, or mechanical mechanisms, which are generally time-consuming and energy-consuming [6].

Regarding thermal treatments, dry heat ( $> 180\text{ }^{\circ}\text{C}$ ), hot water and steam ( $130\text{--}150\text{ }^{\circ}\text{C}$ ) are the most commonly applied. Although thermal methods do not present residues of environmental hazards, some spores are resistant to heat [6]. Moreover, they require a lot of energy and long treatment times, being only possible to employ materials with high thermal resistance.

Chemical treatments such as hydrogen peroxide, ozone, peracetic acid or ethylene oxides could be toxic for people when used wrongly. Besides, they are known to leave residues on the treated surfaces causing resistances to bacteria and increasing their economic cost [6–8]. Additionally, there are some chemicals used in the food industry which could react with organic matter present on the surface reducing the efficacy (i.e. chlorine-based sanitizers) [9].

Therefore, there is a need to identify and develop new strategies, based on non-thermal physical mechanisms. Among these, ultraviolet, high hydrostatic pressure, ionizing or electron beam radiation and pulsed light have been effectively proven [10]. These technologies work at high efficiency requiring less energy input compared to the above technologies, and almost no residue or process waste is produced.

Cold Atmospheric Pressure Plasma (CAP) treatments may be a viable option for microbial inactivation, as they have antimicrobial active components, such as reactive oxygen and nitrogen species (RONS), ultraviolet radiation, electrons, radicals, ions, excited molecules and electromagnetic fields [11]. Several of these components have been found to be effective, thus it is reasonable to assume that their synergistic action could be highly beneficial. Moreover, these types of treatments represent an economical, green, and safe technology, which can allow the avoidance or reduction of traditional chemical sanitizers [12].

By virtue of the above considerations, it is of great interest to investigate the potential use of cold plasmas for the decontamination of products, instruments, and packaging in the food industry. Besides, some authors studied this technology for food-packaging decontamination [13–15].

In particular, many authors investigated the potential use of DBD (Dielectric Barrier Discharge) and SDBD (Surface Dielectric Barrier Discharge) for the decontamination of food packaging and food-processing surfaces [1, 16, 17].

Among the characteristics of DBD, they have two electrodes and at least one dielectric layer between them. They provide a huge homogenous plasma area, being easy to use, stable, and affordable, making them suitable for surface treatment [18]. Moreover, thin films

can easily fit in the gap (0.1 mm to several centimeters) between the DBD electrodes, thus being especially appropriate to be treated by DBD sources.

Additionally, the features of these devices rely on the electrode geometries and dimensions, materials selected, gas characteristics, and the applied electric field. Many different setups are possible, varying these parameters.

SDBD is one of the several setups possible for DBD. There, both electrodes are in contact with the dielectric material, and plasma is generated on the ground electrode surface. The main advantage of SDBD configuration, as opposed to DBD presenting a gap between electrodes, is the fact that the treated surface is kept outside of the electrical circuit, and, therefore, the working of the plasma source is almost independent of the treated material. Another benefit of both DBD and SDBD is that they can easily work using air as process gas. Specifically, the use of ambient air rather than expensive technical gases makes the difference from an industrial perspective [18].

The present work has characterized an SDBD plasma source from an electrical, chemical, and physical point of view. Moreover, its anti-bacterial efficacy has been evaluated against *Staphylococcus epidermidis* inoculated on polypropylene samples.

## Materials and Methods

### Plasma System

A Large Area Surface Dielectric Barrier Discharge (LA-SDBD, AlmaPlasma s.r.l., Bologna, Italy) was used to achieve indirect treatments [19].

The main components of the source are illustrated in Fig. 1. Four rectangular high-voltage electrodes (115 cm<sup>2</sup> each) were embedded in resin, and they were cooled by a glycol flux provided by a commercial cooling system (EXT-440, Koolance, USA). A dielectric layer made of mica (2 mm thick) was in contact with both the high-voltage electrodes and

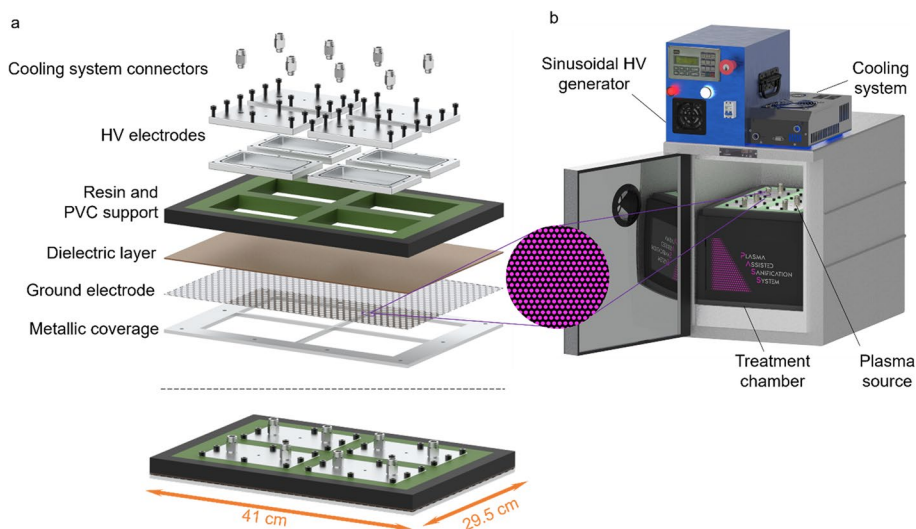


**Fig. 1** **a** Plasma source components: exploded and assembly view; **b** plasma system components

ground electrodes. The latter, consisting of a perforated plate, was kept in place thanks to a metallic coverage. Plasma was generated in correspondence with the holes of the ground electrode, as depicted in Fig. 1. The plasma source was fed by a sinusoidal high-voltage generator (AlmaPlasma s.r.l., Bologna, Italy) working with a peak-to-peak voltage of 14 kV and a frequency of 23 kHz.

The plasma source constituted the lid of a PVC treatment chamber with a volume of 17.5 L. During treatments, the plasma source closed the treatment chamber, in order to create a confined atmosphere.

The source was designed to produce reactive species at atmospheric pressure, within the temperature and relative humidity ranges of 5–40 °C and 0–90%, respectively.

## Microbial Strain and Sample Inoculation/Recovery

Circular polypropylene (PP) samples (Ø 2.5 cm) were contaminated.

*Staphylococcus epidermidis* ATCC12228 was selected as the target microorganism. Bacteria inoculum was cultured in tryptic soy agar (TSA, VWR International, Belgium) for 24 h at 37 °C. After that, the master suspension was adjusted at  $OD_{600\text{nm}}=0.2$  ( $10^7$ – $10^8$  CFU/mL) and assessed with a spectrophotometer (FullTech Instruments, Italy) [20].

Before treatments, PP samples were sterilized with ethanol 70% (Sigma-Aldrich, USA) before 5 min under UV light (Bio II Advance, Telstar, Japan). The master suspension was used in order to inoculate the PP samples with 20 drops of 1 µL (treatment samples and control samples). For bacteria recovery, treated and control samples were submerged for 2 min in PBS (Corning, USA) + 1% Tween 80 solution (Sigma-Aldrich, USA) and dilutions and spreading on agar plates were done. Then, the samples were kept for 24 h at 37 °C and recounted. Control samples followed the same procedure as plasma-treated samples but with plasma OFF.

The next formula was used to evaluate the antibacterial activity of plasma treatments after recovery steps:

$$\text{Log reduction} = \log N_0 - \log N_t$$

where  $N_0$  and  $N_t$  are the number of colony-forming units of control and plasma treated, respectively.

## Analytical Determinations

### Electrical Characterization

In order to calculate the mean electrical power, voltage, and current waveforms were acquired. A voltage probe (P6015A, 1000×,  $R_p=100\text{ M}\Omega$ , Tektronix, USA) and a current probe (Current Monitor 6585, Pearson Electronics, USA) were placed respectively on the high voltage and the ground cable, and they were both connected to a fast oscilloscope (MSO46, Tektronix, USA) for the detection (Fig. 2).

Waveforms were acquired at the beginning and every five minutes of treatment, with a total of seven acquisitions for each 30-min test. Every acquisition had a record length of 180 ms, equal to four periods. Three tests were performed.

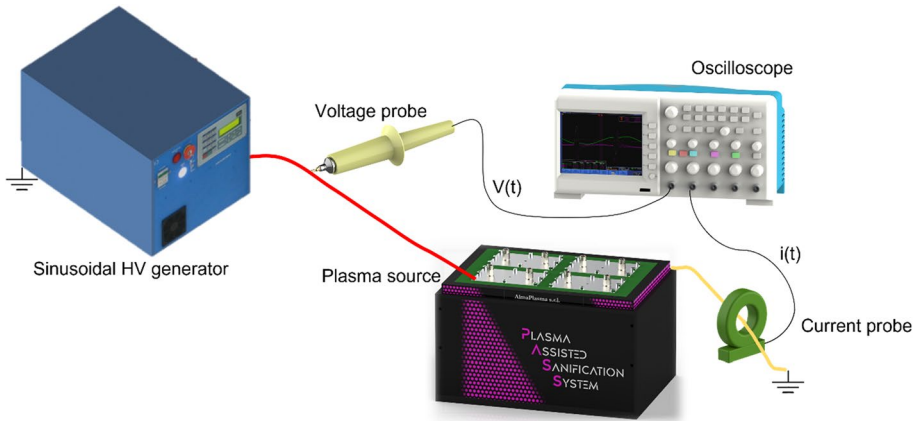


**Fig. 2** Setup for voltage and current waveforms acquisition

Voltage and current values were used to calculate the electrical power at each time step on the basis of Ohm’s law:

$$P(t) = V(t)*I(t)$$

where  $P$  is the electrical power,  $V$  is the voltage, and  $I$  the current.

The average power was calculated over the whole record length for each acquisition, as follows:

$$P_{average} = \frac{1}{T} \int_0^T P(t)dt$$

where the average power ( $P_{average}$ ) is equal to the time integral of the power at each time step ( $\int_0^T P(t)dt$ ), divided by the total amount of time ( $T$ , record length).

The calculation of the average power consumption is useful in order to calculate the specific power density ( $SPD$ ) characteristic of the two duty cycles, by dividing the average power ( $P_{average}$ ) by the plasma generation area ( $A$ ):

$$SPD = \frac{P_{average}}{A}$$

where  $A$  should be calculated as the multiplication of the total surface of the high voltage electrodes ( $S$ ) and the empty coefficient of the ground electrode ( $e=0.33$ ), since plasma is generated only in the holes of the perforated plate, as already mentioned.

$$A = S*e$$

For the plasma source used in this study, the plasma generation area resulted equal to 151.8 cm<sup>2</sup>.

## Optical Absorption Spectroscopy (OAS) and Data Processing

An Optical Absorption Analysis has been performed in order to understand the reactive species kinetics inside the treatment chamber. Two reactive species were chosen: ozone ( $O_3$ ) and nitrogen dioxide ( $NO_2$ ). Their kinetics were detected during 30-min treatments with different plasma conditions.

Two different optical paths were selected, in order to acquire the kinetics at two different distances from the plasma generation region, corresponding to the two positions later illustrated.

Optical Absorption Spectroscopy (OAS) is based on the Lambert–Beer law, which states that it is possible to quantify the number of a specific type of molecule by measuring the absorption of certain specific wavelengths. The light intensity of a beam passing through a region where there are molecules that absorb the characteristic wavelength of the beam is attenuated proportionally to the amount of molecules present in that region.

A similar setup for OAS was previously described by Simoncelli et al. [21] (Fig. 3). The light source used for ozone detection was a deep-UV led lamp (LEDMOD255.001.V2, Omicron Laserage, Germany), set at a wavelength of 255 nm. For nitrogen dioxide detection, a commercial led with an emission wavelength of 400 nm has been used. The light beam was focused in both cases with a lens in order to obtain a parallel beam under the mesh and to be able to collect it into a 500 mm spectrometer (Acton SP2500i, Princeton Instruments).

OAS acquisitions were performed using a grating with a resolution of  $150\text{ mm}^{-1}$  or  $1800\text{ mm}^{-1}$ , respectively, when detecting ozone or nitrogen dioxide, and setting a width of  $10\text{ }\mu\text{m}$  for the inlet slit of the spectrometer. With the aim of achieving fast acquisition with a time resolution of 40 ms, a photomultiplier tube (PMT—PD439, Princeton Instruments) connected to a fast oscilloscope (MSO46, Tektronix, USA) was used as a detector. The PMT amplification factor was fixed at 585 and kept constant for all measurements. Each measurement was repeated three times.

The concentration of RONS in the closed chamber can be calculated spectrally by resolving the collected beam and taking the Lambert–Beer Law into account:

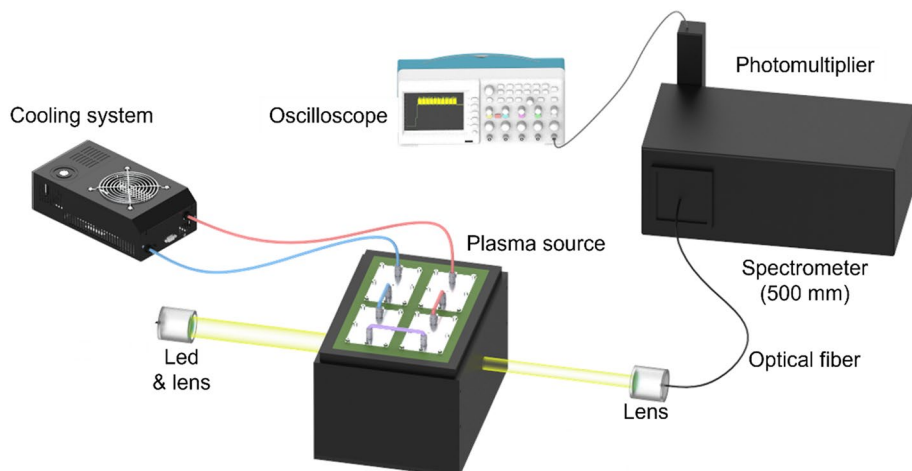


**Fig. 3** Schematic of the experimental setup for optical absorption spectroscopy

**Table 1** Selected wavelengths and absorption cross-sections of the O<sub>3</sub> and NO<sub>2</sub> (cm<sup>2</sup>)

| Selected wavelength (nm) | O <sub>3</sub> cross-section | NO <sub>2</sub> cross-section |
|--------------------------|------------------------------|-------------------------------|
| 253 ± 1.2                | (1.12 ± 0.02)E-17            | (1.1 ± 0.3)E-20               |
| 400 ± 1.2                | (1.12 ± 0.08)E-23            | (6.4 ± 0.2)E-19               |

**Table 2** Plasma treatments conditions

| Treatment number     | 1   | 2   | 3    | 4    | 5   | 6   | 7    | 8    |
|----------------------|-----|-----|------|------|-----|-----|------|------|
| Duty cycle 10–100%   | 10% | 10% | 100% | 100% | 10% | 10% | 100% | 100% |
| Gap (cm)             | 20  | 4   | 20   | 4    | 20  | 4   | 20   | 4    |
| Treatment time (min) | 30  | 30  | 30   | 30   | 30  | 30  | 30   | 30   |
| Fan ON–OFF           | OFF | OFF | OFF  | OFF  | ON  | ON  | ON   | ON   |

Each treatment consisted of a group of three samples and was performed three times

$$\frac{I}{I_0} = e^{(-L\sigma n)}$$

where the concentration of the absorbers ( $n$ ), which has to be quantitatively evaluated, is correlated with the light absorbed after an optical path length ( $L$ ) and expressed as the ratio between the initial light intensity ( $I_0$ ) and the residual light intensity ( $I$ ) after passing through the absorbers region. The absorption cross-section ( $\sigma$ ) is a function of the light wavelength ( $\sigma = \sigma(\lambda)$ ). In the experiments, the optical path was 25 cm long.

The wavelengths selected to perform the acquisitions and the relative absorption cross-sections for the absorbers (O<sub>3</sub> and NO<sub>2</sub>) are reported in Table 1. These wavelengths were defined, in accordance with Moiseev [22], to maximise the absorption of the molecules relevant to our study while minimising the contribution, and thus the disturbance, of other absorbing molecules. The contribution of background radiation is subtracted from the measured values of light intensity.

## Temperature Measurements

The temperature inside the treatment chamber during the treatment was measured. Two commercial fibre-optic sensors (MultiSens, OpSens, Canada) were placed inside the treatment chamber in the same positions chosen for the sample placement. The temperature was monitored for 30 min of plasma treatment under all the different operating conditions. Each measurement was repeated three times. The probes were connected to a detection device (MultiSens, OpSens, Canada) for data acquisition.

## Plasma Treatments

The contaminated samples were located inside the treatment chamber and laid on plastic plates. Eight different treatments were carried out depending on the duty cycle (DC), fan mode, and gap (i.e., the distance between samples and plasma generation region) selected (Table 2). Two different sample positions were chosen, the first one centred on

the bottom of the treatment chamber (gap equal to 20 cm) and the second one in proximity to the plasma discharge (4 cm under the ground electrode). They will be hereafter called “Position 1” and “Position 2”, respectively, as shown in Fig. 4.

The duty cycle (i.e., the ratio between the on-time of the discharge and the sum of on and off time) was either 10% or 100%.

A fan has been placed inside the treatment chamber in order to evaluate the effect of a turbulent atmosphere. All the tests were performed, either with the fan working or not. The fan was located near a short side of the chamber, parallel to it, and facing the other short side, as shown in Fig. 4.

## Statistical Analysis

All experiments were repeated three times. Results are presented as mean value and standard error. In order to assess statistically significant differences among different results, a Student’s test was performed ( $p$ -value < 0.001). Statistical analysis of microbiological data was performed using Statgraphics Centurion software (v19, The Plains, United States).

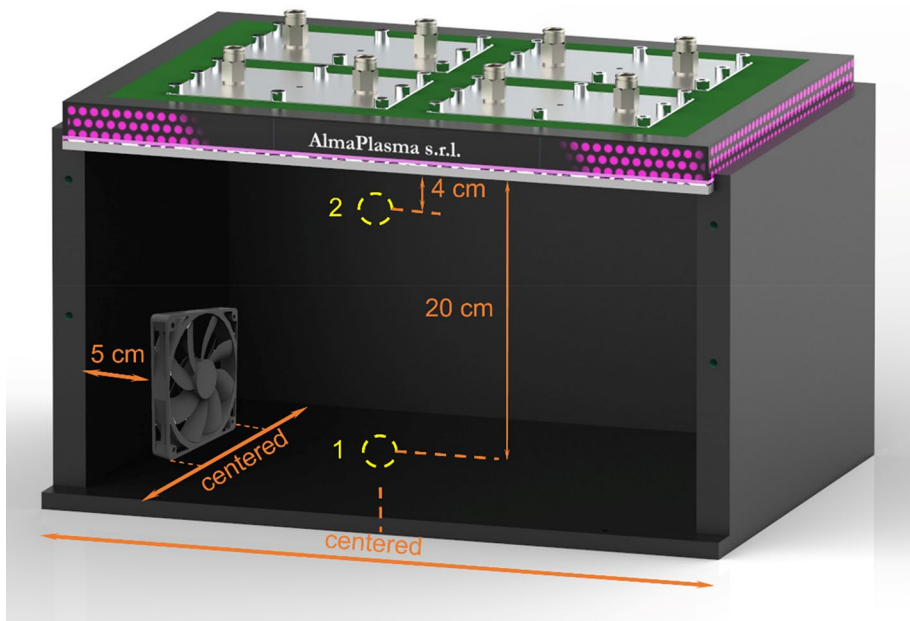


**Fig. 4** Views of the plasma system showing the two chosen positions for the tests, indicated by the circles, and the position of the fan inside the treatment chamber (placed 5 cm apart from one of the short sides of the chamber, centred with respect to it, moving the air toward the other short side)



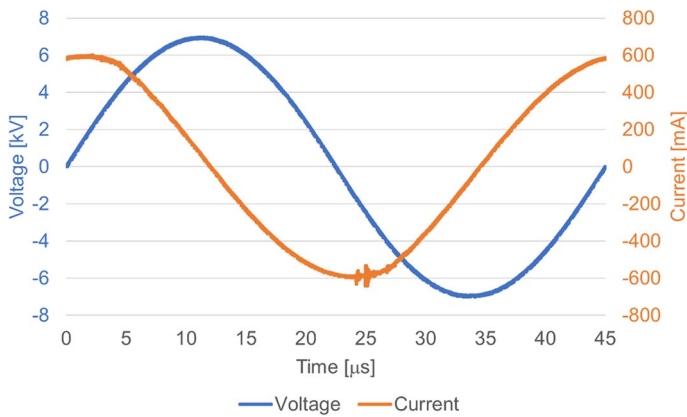


**Fig. 5** Voltage (blue) and current (orange) waveforms acquired during 45  $\mu\text{s}$  of discharge with DC 100% (Color figure online)

**Table 3** Average power and SPD results

| DC (%) | Average power [W] | SPD [ $\text{W cm}^{-2}$ ] | Regime          |
|--------|-------------------|----------------------------|-----------------|
| 10     | $19 \pm 1.6$      | 0.13                       | Ozone           |
| 100    | $190 \pm 16.6$    | 1.25                       | Nitrogen oxides |

## Results and Discussion

### Electrical Characterization

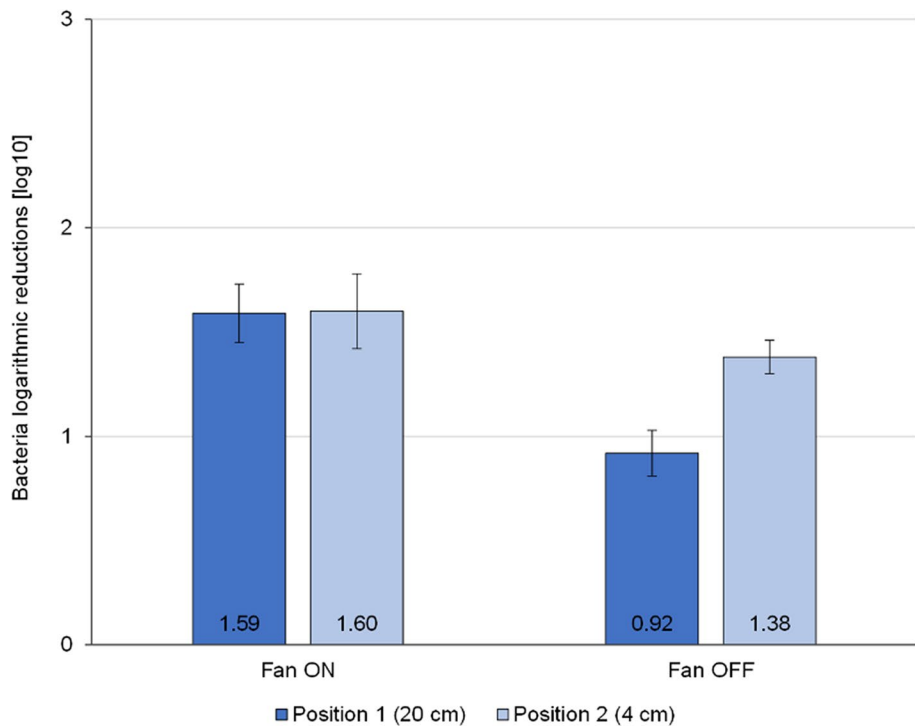
Figure 5 shows voltage and current waveforms recorded for each duty cycle (10 and 100%). From those results the mean electric power was calculated as previously explained, resulting in values of  $19 \pm 16.6$  W and  $190 \pm 1.6$  W for DC 10 and DC 100% respectively.

Table 3 shows the SPD values. With DC 10%, the SPD was about  $0.1 \text{ W cm}^{-2}$ , which is the value identified by the literature [21, 22] as the threshold between the ozone regime ( $\text{SPD} < 0.1 \text{ W cm}^{-2}$ ) and the nitrogen oxides regime. When DC was set at 100%, the source was working in a nitrogen oxides regime.

### Bacteria Inactivation

This section shows the results of bacteria inactivation after each plasma treatment.

Figure 6 illustrates the inactivation rates achieved with plasma treatments in the ozone regime. When comparing fan ON and OFF, for position 1 plasma treatments achieved bacteria reductions of  $1.59 \pm 0.42$  log and  $0.92 \pm 0.34$  log, with fan ON and OFF respectively. While the inactivation obtained for position 2 was  $1.6 \pm 0.53$  log with fan ON and  $1.38 \pm 0.23$  log with fan OFF. They showed no statistically significant differences when comparing fan ON and OFF for each gap, which suggested a homogeneous distribution of the reactive species within the treatment chamber. On the other hand, when doing an evaluation about the two positions where the samples



**Fig. 6** *Staphylococcus epidermidis* inactivation rates with fan ON and fan OFF and sample position 1 and 2 for DC 10%; no statistically significant differences were observed among the different conditions

were laid, without changing the fan mode, no statistically significant differences were shown, which is in line with the last suggestion. Since the position of the sample did not affect the final inactivation rates, it was proposed the idea of an equal mixture of RONS inside the chamber. Furthermore, Fig. 7 shows *S. epidermidis* inactivation relative to each plasma treatment condition, when operating in NO<sub>x</sub> regimen. For instance, when the fan was ON and the samples were in position 1,  $1.51 \pm 0.59$  log reduction was reached and  $1.24 \pm 0.96$  log reduction with the fan OFF. No statistically significant differences were observed among any plasma treatment, neither comparing sample position nor comparing fan mode.

Those results are in accordance with the ones of other authors such as Min [23], who observed 0.9 log CFU/tomato of *Salmonella* wherever the tomatoes samples were inside the plasma treatment chamber, either the bottom layer or the top layer. Nevertheless, a study carried out by Miao [24], using a DBD plasma system without a treatment chamber, investigated how the gap affected the inactivation rate. They showed that the higher the gap (cm) the lower the inactivation values which is not in agreement with the results of this paper. These differences may be due to the fact that in this work, a plasma treatment chamber was used and RONS could be kept inside the chamber. However, without a chamber, RONS could be dispersed throughout the ambient atmosphere, not directly contacting the bacteria sample.

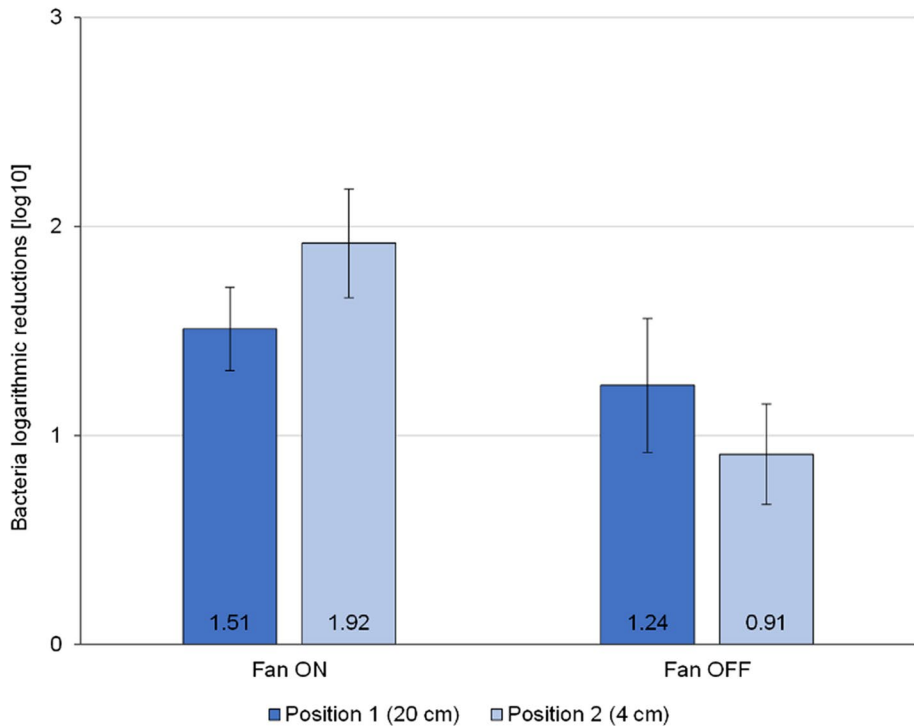


**Fig. 7** *Staphylococcus epidermidis* inactivation rates with fan ON and fan OFF and sample position 1 and 2) for DC 100%; no statistically significant differences were observed among the different conditions

## Reactive Species Concentrations

OAS measurements of reactive species kinetics in the different conditions were elaborated in order to calculate the mean concentrations in correspondence of each optical path during the whole treatment time. Results of calculations with DC 10 and 100% are respectively shown in Figs. 8 and 9.

Ozone concentration in the nitrogen regime was also measured by OAS resulting in not significant values (data not shown). Regarding nitrogen dioxide in the ozone regime, the measured concentrations were considered irrelevant. The presented results suggest that the reactive species concentration inside the treatment chamber is homogeneous, since no statistically significant difference was observed among the results relative to different positions, even without the gas mixing provided by the fan. Indeed, the results obtained in the two different positions were equal from a statistical point of view even in the “fan OFF” condition.

## Temperature Profiles

In order to evaluate the plasma treatment influence on the temperature of the atmosphere inside the chamber, thermal measurements with the two fan modes were carried out. As

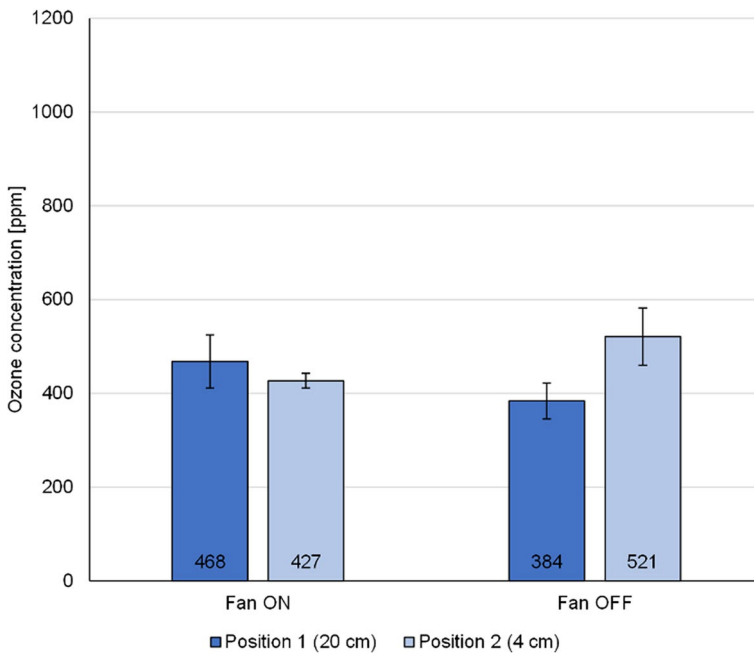


**Fig. 8** Mean ozone concentration in the two selected positions over 30-min treatments (each result is the average of three replicates) with DC 10%; no statistically significant differences were observed among the different conditions

Figs. 10 and 11 show, the temperature increase was higher in the case of NO<sub>x</sub> regime, for both the investigate positions and the fan modes. This fact is an expected result, since the higher DC has the effect of a higher power consumption, and thus Joule heating of the plasma source. Furthermore, it was also expected to observe a greater temperature increase in correspondence with position 2, due to the reduced distance from the ground electrode. However, the greatest increase observed was equal to about 10 °C with respect to the ambient temperature (Fig. 11b, DC 100%).

The results suggested that the temperature reached inside the treatment chamber, cannot significantly influence the microbial cells viability, since its value was holding below 40 °C. That temperature is much higher than the temperature range of growth of *Staphylococci* strains, which is 6.5–46 °C [25]. Thus, it is suggested that the inactivation rate achieved after plasma treatments was not caused by a thermal effect.

Furthermore, the temperature results indicate that the process could be suitable for heat-sensitive materials, such as polymeric packaging.

## Conclusions

In the present work, the effectiveness of an LA-SDBD was studied for decontaminating food packaging surfaces. Different parameters, such as the gap (20 and 4 cm) or the fan mode (ON and OFF), were investigated during the plasma treatment. Biological results showed bacterial inactivations of 1–2 logarithmic reductions, which can be considered

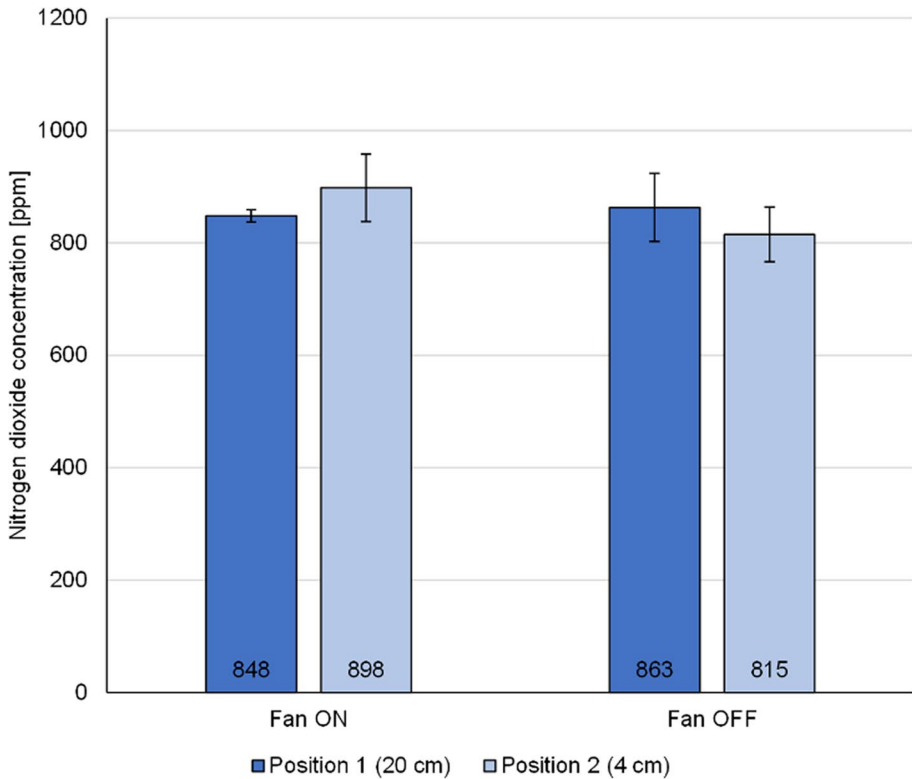


**Fig. 9** Mean nitrogen dioxide concentration in the two selected positions over 30-min treatments (each result is the average of three replicates) with DC 100%; no statistically significant differences were observed among the different conditions

as a preliminary result for further process optimization. It was also suggested a homogeneous RONS diffusion inside the treatment chamber since there were no statistically significant differences in terms of bacteria inactivation for each plasma treatment condition. This fact was also corroborated by OAS analysis which illustrated no statistically significant differences for  $O_3$  and  $NO_2$  regardless of the operating condition applied. It is thus possible to conclude that the device can effectively work in both operating conditions. Moreover, it has been verified that the anti-bacterial action is unvaried in different positions inside the 17.5 L treatment chamber. This statement suggests that three-dimensional objects could be sanitized with high efficacy.

Furthermore, since the samples were not in direct contact with plasma and there was a slight temperature increase, it could be assumed that reactive oxygen and nitrogen species play a key role in the antimicrobial efficacy of the plasma source used. Finally, it is remarkable that the presented homogeneous results were obtained inside a treatment chamber with a volume of 17.5 L and with a plasma source characterized by a large electrode area. According to the authors' knowledge, this is the plasma system intended for food packaging decontamination with the largest discharge area and one of the largest volumes in the literature.

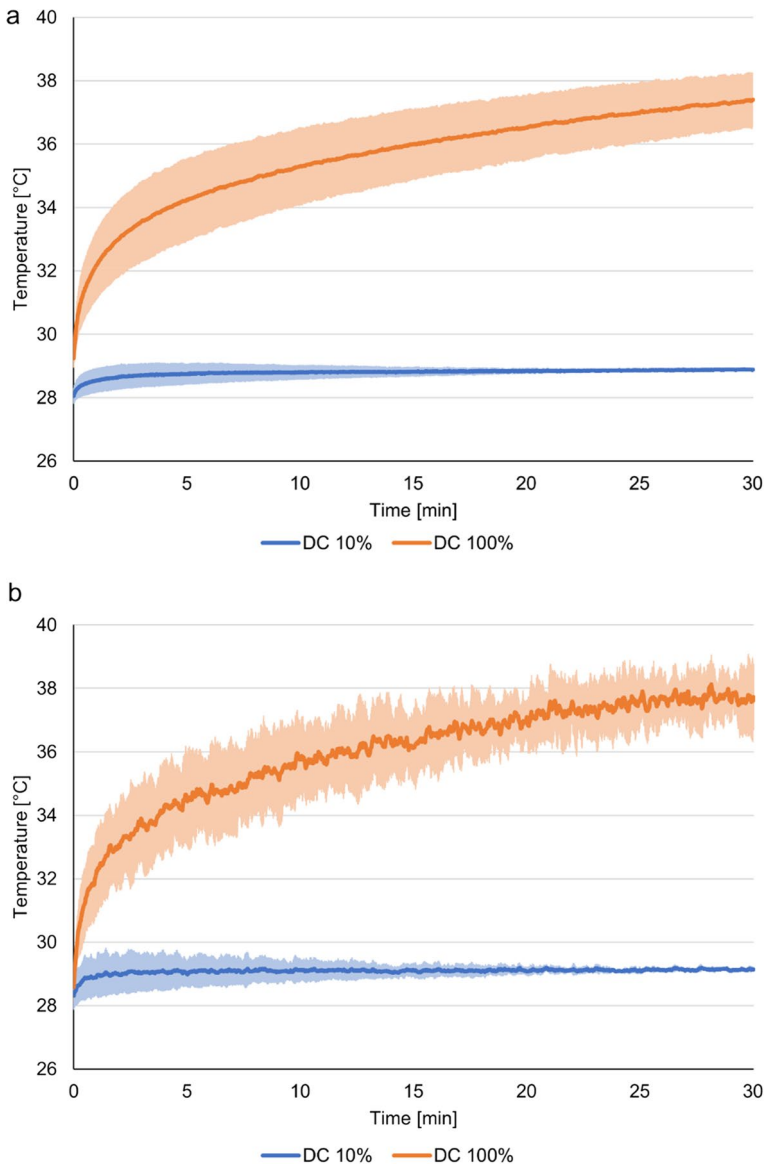


**Fig. 10** Temperature profiles inside the treatment chamber with fan OFF at distances of 20 cm (position 1, **a**) and 4 cm (position 2, **b**) from the ground electrode

Future research may include the optimization of the plasma system and the process in general, the antimicrobial efficacy evaluation on different types of microorganisms and the evaluation of potential modification of PP matrix induced by CAP treatment.

In conclusion, disinfecting food packaging and tools by LA-SDBD could be a sustainable and cost-efficient electricity-based solution for food chain contamination and thus for avoiding and reducing foodborne diseases.

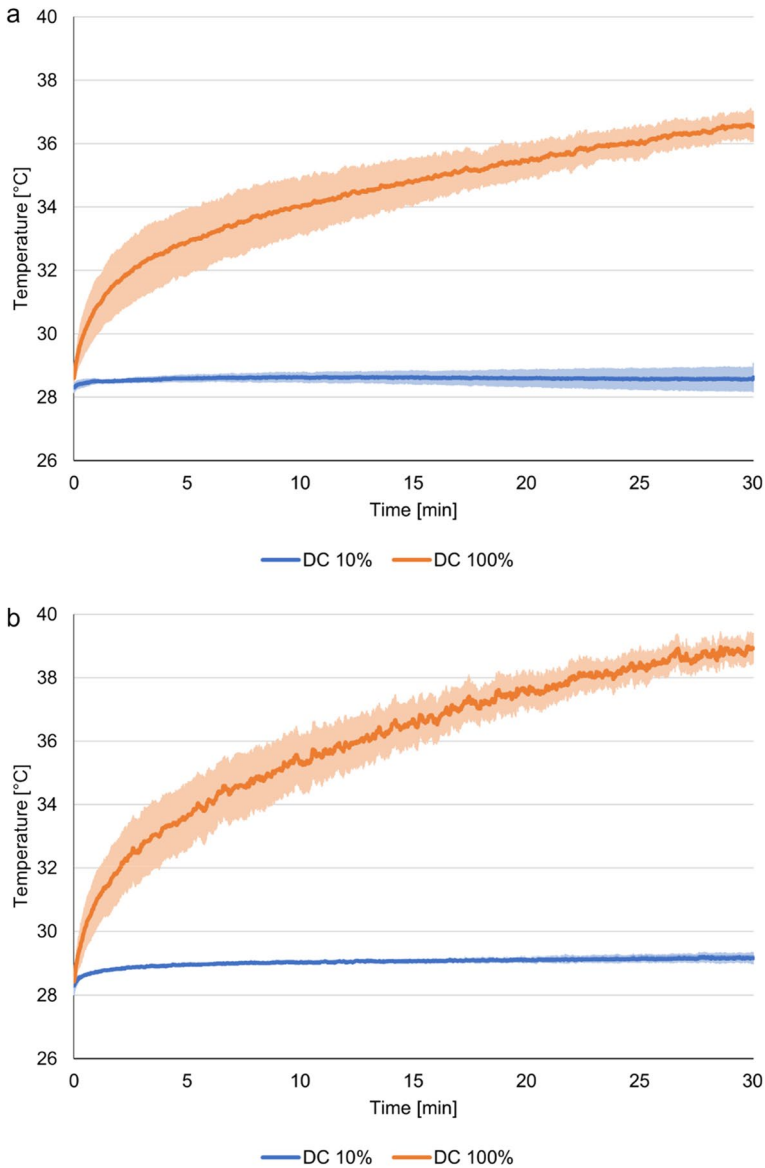


**Fig. 11** Temperature profiles inside the treatment chamber with fan ON at distances of 20 cm (position 1, **a**) and 4 cm (position 2, **b**) from the ground electrode

**Acknowledgements** The author Sainz-García, A. is thankful to the program of pre-doctoral contracts for the training of research staff that is funded by the Spanish Ministry of Science and Innovation and the COST Action CA20114 PlasTHER, supported by COST (European Cooperation in Science and Technology—<https://www.cost.eu>). The PhD scholarship of the author Maccaferri, C. was funded by the European Union—NextGenerationEU through the Italian Ministry of University and Research under PNRR—Mission 4 Component 2, Investment 3.3 “Partnerships extended to universities, research centres, companies and funding of basic research projects” D.M. 352/2021-CUP J33C22001330009.

**Author Contribution** C.M.: Conceptualization, Methodology, Validation, Formal analysis, Investigation, Data curation, Writing—original draft preparation, Writing—review and editing, Visualization. A.S.G.: Methodology, Validation, Formal analysis, Investigation, Data curation, Writing—original draft preparation, Writing—review and editing, Visualization. F.C.: Methodology, Validation, Formal analysis, Investigation, Writing—review and editing. M.G.: Writing—review and editing, Supervision, Funding acquisition. F.A.E.: Writing—review and editing, Supervision, Funding acquisition. R.L.: Conceptualization, Methodology, Resources, Writing—review and editing, Supervision, Project administration, Funding acquisition.

**Funding** Open access funding provided by Alma Mater Studiorum - Università di Bologna within the CRUI-CARE Agreement. This work has been funded by MCIN/AEI/<https://doi.org/10.13039/501100011033> and the “European Union NextGenerationEU/PRTR” through Grants PID2019-105367RB, PID2020-11365RB-C21 and PDC2022-133242-I00.

## Declarations

**Conflict of Interest** None.

**Open Access** This article is licensed under a Creative Commons Attribution 4.0 International License, which permits use, sharing, adaptation, distribution and reproduction in any medium or format, as long as you give appropriate credit to the original author(s) and the source, provide a link to the Creative Commons licence, and indicate if changes were made. The images or other third party material in this article are included in the article’s Creative Commons licence, unless indicated otherwise in a credit line to the material. If material is not included in the article’s Creative Commons licence and your intended use is not permitted by statutory regulation or exceeds the permitted use, you will need to obtain permission directly from the copyright holder. To view a copy of this licence, visit <http://creativecommons.org/licenses/by/4.0/>.

## References

1. Capelli F, Tappi S, Gritti T, et al (2021) Decontamination of food packages from SARS-COV-2 RNA with a cold plasma-assisted system. *Appl Sci* (Switzerland). <https://doi.org/10.3390/app11094177>
2. Godfray H CJ, Crute IR, Haddad L et al (2010) The future of the global food system. *Philos Trans R Soc B: Biol Sci* 365:2769–2777. <https://doi.org/10.1098/rstb.2010.0180>
3. World Health Organization—23 million people falling ill from unsafe food each year in Europe is just the tip of the iceberg (2019). <https://www.who.int/news/item/05-06-2019-23-million-people-falling-ill-from-unsafe-food-each-year-in-europe-is-just-the-tip-of-the-iceberg>. Accessed 23 Mar 2023
4. Farias A da S, Akutsu R de CC de A, Botelho RBA, Zandonadi RP (2019) Good practices in home kitchens: construction and validation of an instrument for household food-borne disease assessment and prevention. *Int J Environ Res Public Health*. <https://doi.org/10.3390/ijerph16061005>
5. Lorenzo JM, Munekata PE, Dominguez R, et al (2018) Main groups of microorganisms of relevance for food safety and stability: general aspects and overall description. *Innov Technol Food Preser* 53–107. <https://doi.org/10.1016/B978-0-12-811031-7.00003-0>
6. Ansari IA, Datta AK (2003) An overview of sterilization methods for packaging materials used in aseptic packaging systems. *Food Bioprod Process* 81:57–65. <https://doi.org/10.1205/096030803765208670>
7. Khadre MA, Yousef AE (2001) Decontamination of a multilaminated aseptic food packaging material and stainless steel by ozone. *J Food Saf* 21:1–13. <https://doi.org/10.1111/j.1745-4565.2001.tb00304.x>
8. Office of the Federal Register National Archives and Records Administration (1939; Revised April 2021). Food and Drug Administration, Department of Health and Human Services. 21 CFR 170.3
9. Virto R, Mañas P, Álvarez I et al (2005) Membrane damage and microbial inactivation by chlorine in the absence and presence of a chlorine-demanding substrate. *Appl Environ Microbiol* 71:5022–5028. <https://doi.org/10.1128/AEM.71.9.5022-5028.2005>
10. Prakasam M, Largeteau A (2017) Flexible packaging for nonthermal decontamination by high hydrostatic pressure. Elsevier
11. Liao X, Liu D, Xiang Q et al (2017) Inactivation mechanisms of non-thermal plasma on microbes: a review. *Food Control* 75:83–91. <https://doi.org/10.1016/j.foodcont.2016.12.021>



12. Puligundla P, Lee T, Mok C (2016) Inactivation effect of dielectric barrier discharge plasma against foodborne pathogens on the surfaces of different packaging materials. *Innov Food Sci Emerg Technol* 36:221–227. <https://doi.org/10.1016/J.IFSET.2016.06.027>
13. Ucar Y, Ceylan Z, Durmus M et al (2021) Application of cold plasma technology in the food industry and its combination with other emerging technologies. *Trends Food Sci Technol* 114:355–371. <https://doi.org/10.1016/j.tifs.2021.06.004>
14. Sani IK, Aminoleslami L, Mirtalebi SS et al (2023) Cold plasma technology: applications in improving edible films and food packaging. *Food Packag Shelf Life* 37:101087. <https://doi.org/10.1016/j.fpsl.2023.101087>
15. Kordová T, Scholtz V, Khun J, et al (2018) Inactivation of microbial food contamination of plastic cups using nonthermal plasma and hydrogen peroxide. *J Food Qual.* <https://doi.org/10.1155/2018/5616437>
16. Pina-Perez MC, Martinet D, Palacios-Gorba C, et al (2020) Low-energy short-term cold atmospheric plasma: controlling the inactivation efficacy of bacterial spores in powders. *Food Res Int.* <https://doi.org/10.1016/j.foodres.2019.108921>
17. Timmons C, Pai K, Jacob J et al (2018) Inactivation of *Salmonella enterica*, Shiga toxin-producing *Escherichia coli*, and *Listeria monocytogenes* by a novel surface discharge cold plasma design. *Food Control* 84:455–462. <https://doi.org/10.1016/j.foodcont.2017.09.007>
18. Katsigiannis AS, Bayliss DL, Walsh JL (2022) Cold plasma for the disinfection of industrial food-contact surfaces: an overview of current status and opportunities. *Compr Rev Food Sci Food Saf* 21:1086–1124
19. Molina-Hernandez JB, Capelli F, Laurita R, et al (2022) A comparative study on the antifungal efficacy of cold atmospheric plasma at low and high surface density on *Aspergillus chevalieri* and mechanisms of action. *Innov Food Sci Emerging Technol.* <https://doi.org/10.1016/j.ifset.2022.103194>
20. Yang C, Mamouni J, Tang Y, Yang L (2010) Antimicrobial activity of single-walled carbon nanotubes: length effect. *Langmuir* 26:16013–16019. <https://doi.org/10.1021/la103110g>
21. Simoncelli E, Schulpen J, Barletta F, et al (2019) UV-VIS optical spectroscopy investigation on the kinetics of long-lived RONS produced by a surface DBD plasma source. *Plasma Sour Sci Technol.* <https://doi.org/10.1088/1361-6595/ab3c36>
22. Moiseev T, Misra NN, Patil S, et al (2014) Post-discharge gas composition of a large-gap DBD in humid air by UV-Vis absorption spectroscopy. *Plasma Sour Sci Technol.* <https://doi.org/10.1088/0963-0252/23/6/065033>
23. Min SC, Roh SH, Niemira BA et al (2018) In-package atmospheric cold plasma treatment of bulk grape tomatoes for microbiological safety and preservation. *Food Res Int* 108:378–386. <https://doi.org/10.1016/j.foodres.2018.03.033>

24. Miao H, Yun G (2011) The sterilization of *Escherichia coli* by dielectric-barrier discharge plasma at atmospheric pressure. *Appl Surf Sci* 257:7065–7070. <https://doi.org/10.1016/j.apsusc.2011.03.014>
25. Onyango LA, Dunstan RH, Gottfries J et al (2012) Effect of low temperature on growth and ultra-structure of *Staphylococcus* spp. *PLoS ONE* 7:1–10. <https://doi.org/10.1371/journal.pone.0029031>

**Publisher's Note** Springer Nature remains neutral with regard to jurisdictional claims in published maps and institutional affiliations.

## Authors and Affiliations

Caterina Maccaferri<sup>1</sup>  · Ana Sainz-García<sup>2</sup>  · Filippo Capelli<sup>1</sup>  ·  
Matteo Gherardi<sup>1,3</sup>  · Fernando Alba-Elías<sup>2</sup>  · Romolo Laurita<sup>1,4</sup> 

✉ Romolo Laurita  
romolo.laurita@unibo.it

Caterina Maccaferri  
caterina.maccaferri3@unibo.it

Ana Sainz-García  
ana.sainz@unirioja.es

Filippo Capelli  
Filippo.capelli@unibo.it

Matteo Gherardi  
matteo.gherardi4@unibo.it

Fernando Alba-Elías  
fernando.alba@unirioja.es

- <sup>1</sup> Department of Industrial Engineering, Alma Mater Studiorum, Università di Bologna, Bologna, Italy
- <sup>2</sup> Department of Mechanical Engineering, Universidad de La Rioja, Logroño, Spain
- <sup>3</sup> Advanced Mechanics and Materials, Interdepartmental Center for Industrial Research (AMM-ICIR), Alma Mater Studiorum, Università di Bologna, Bologna, Italy
- <sup>4</sup> Interdepartmental Centre for Industrial Research Health Sciences and Technologies, Alma Mater Studiorum, Università di Bologna, Ozzano Dell'Emilia, Italy